

1 **dsMTL - a computational framework for privacy-preserving,  
2 distributed multi-task machine learning**

3 Han Cao<sup>1#</sup>, Youcheng Zhang<sup>2#</sup>, [alphabetical order starts] Jan Baumbach<sup>3,4</sup>, Paul R Burton<sup>5</sup>, Dominic  
4 Dwyer<sup>6</sup>, Nikolaos Koutsouleris<sup>6</sup>, Julian Matschinske<sup>3</sup>, Yannick Marcon<sup>7</sup>, Sivanesan Rajan<sup>1</sup>, Thilo Rieg<sup>1</sup>,  
5 Patricia Ryser-Welch<sup>5</sup>, Julian Späth<sup>3</sup>, [alphabetical order ends], The COMMITMENT consortium, Carl  
6 Herrmann<sup>2\*</sup>, Emanuel Schwarz<sup>1\*</sup>

7 <sup>1</sup> Department of Psychiatry and Psychotherapy, Central Institute of Mental Health, Medical Faculty Mannheim,  
8 Heidelberg University, Mannheim, Germany.

9 <sup>2</sup> Health Data Science Unit, Medical Faculty Heidelberg & BioQuant, Heidelberg, 69120, Germany.

10 <sup>3</sup> Chair of Computational Systems Biology, University of Hamburg, Hamburg, Germany

11 <sup>4</sup> Computational Biomedicine Lab, Department of Mathematics and Computer Science, University of Southern  
12 Denmark, Odense, Denmark

13 <sup>5</sup> Population Health Sciences Institute, Newcastle University, Newcastle upon Tyne, United Kingdom

14 <sup>6</sup> Department of Psychiatry and Psychotherapy, Section for Neurodiagnostic Applications, Ludwig-Maximilian  
15 University, Munich 80638, Germany.

16 <sup>7</sup> Epigeny, St Ouen, France

17

18

\*To whom correspondence should be addressed: [emanuel.schwarz@zi-mannheim.de](mailto:emanuel.schwarz@zi-mannheim.de)

[carl.herrmann@bioquant.uni-heidelberg.de](mailto:carl.herrmann@bioquant.uni-heidelberg.de)

19 <sup>#</sup>These authors contributed equally to the study

20

21

22

23

24

25

26

27

28 **Consortium authors**

29 **The COMMITMENT consortium:**

30 Emanuel Schwarz<sup>1\*</sup>, *[alphabetical order starts]* Dag Alnæs<sup>2</sup>, Ole A. Andreassen<sup>2</sup>, Han Cao<sup>1</sup>, Junfang  
31 Chen<sup>1</sup>, Franziska Degenhardt<sup>3,4</sup>, Daria Doncevic<sup>5</sup>, Dominic Dwyer<sup>6</sup>, Roland Eils<sup>5,7</sup>, Jeanette Erdmann<sup>8</sup>,  
32 Carl Herrmann<sup>5</sup>, Martin Hofmann-Apitius<sup>9</sup>, Nikolaos Koutsouleris<sup>6,10</sup>, Alpha T. Kodamullil<sup>9</sup>, Adyasha  
33 Khuntia<sup>6</sup>, Sören Mucha<sup>8</sup>, Markus M. Nöthen<sup>3,11</sup>, Riya Paul<sup>6</sup>, Mads L. Pedersen<sup>12</sup>, Heribert Schunkert<sup>13</sup>,  
34 Heike Tost<sup>1</sup>, Lars T. Westlye<sup>2,12</sup>, Youcheng Zhang<sup>5</sup>, *[alphabetical order ends]*, Andreas Meyer-  
35 Lindenberg<sup>1\*</sup>

36

37 <sup>1</sup> Department of Psychiatry and Psychotherapy, Central Institute of Mental Health, Medical Faculty Mannheim,  
38 Heidelberg University, Mannheim, Germany.

39 <sup>2</sup> Norwegian Centre for Mental Disorders Research (NORMENT), Division of Mental Health and Addiction, Oslo  
40 University Hospital and Institute of Clinical Medicine, University of Oslo, Oslo, Norway.

41 <sup>3</sup> Institute of Human Genetics, University of Bonn, School of Medicine & University Hospital Bonn, Bonn,  
42 Germany

43 <sup>4</sup> Department of Child and Adolescent Psychiatry, Psychosomatics and Psychotherapy, University Hospital  
44 Essen, University of Duisburg-Essen, Duisburg, Germany

45 <sup>5</sup> Health Data Science Unit, Medical Faculty Heidelberg and BioQuant, Heidelberg, 69120, Germany.

46 <sup>6</sup> Department of Psychiatry and Psychotherapy, Section for Neurodiagnostic Applications, Ludwig-Maximilian  
47 University, Munich 80638, Germany.

48 <sup>7</sup> Center for Digital Health, Berlin Institute of Health and Charité, Berlin, 10117, Germany.

49 <sup>8</sup> Institute for Cardiogenetics, University of Lübeck, DZHK (German Research Centre for Cardiovascular Research),  
50 partner site Hamburg/Lübeck/Kiel, and University Heart Center Lübeck, Lübeck, Germany.

51 <sup>9</sup> Fraunhofer Institute for Algorithms and Scientific Computing (SCAI), Sankt Augustin, 53754, Germany.

52 <sup>10</sup> Max-Planck Institute of Psychiatry, Munich, Germany

53 <sup>11</sup> Department of Genomics, Life & Brain Center, University of Bonn, Bonn, Germany.

54 <sup>12</sup> Department of Psychology, University of Oslo, Oslo, Norway

55 <sup>13</sup> Department of Cardiology, Deutsches Herzzentrum München, Technische Universität München, Munich Heart  
56 Alliance (DZHK), Germany.

57 **Abstract**

58 Multitask learning allows the simultaneous learning of multiple ‘communicating’ algorithms. It is  
59 increasingly adopted for biomedical applications, such as the modeling of disease progression. As data  
60 protection regulations limit data sharing for such analyses, an implementation of multitask learning on  
61 geographically distributed data sources would be highly desirable. Here, we describe the development  
62 of dsMTL, a computational framework for privacy-preserving, distributed multi-task machine learning  
63 that includes three supervised and one unsupervised algorithms. dsMTL is implemented as a library  
64 for the R programming language and builds on the DataSHIELD platform that supports the federated  
65 analysis of sensitive individual-level data. We provide a comparative evaluation of dsMTL for the  
66 identification of biological signatures in distributed datasets using two case studies, and evaluate the  
67 computational performance of the supervised and unsupervised algorithms. dsMTL provides an easy-  
68 to-use framework for privacy-preserving, federated analysis of geographically distributed datasets,  
69 and has several application areas, including comorbidity modeling and translational research focused  
70 on the simultaneous prediction of different outcomes across datasets. dsMTL is available at  
71 <https://github.com/transbioZI/dsMTLBase> (server-side package) and  
72 <https://github.com/transbioZI/dsMTLClient> (client-side package).

73

74

75

76

77

78

79

80 **Introduction**

81 The biology of many human illnesses is encoded in a vast number of genetic, epigenetic, molecular,  
82 and cellular parameters. The ability of Machine Learning (ML) to jointly analyze such parameters and  
83 derive algorithms with potential clinical utility has fueled a massive interest in biomedical ML  
84 applications. One of the fundamental requirements for such ML algorithms to perform well is the  
85 availability of data at a large scale, a challenge of steadily declining importance due to the ever-  
86 increasing availability of biological data<sup>1-3</sup>. As data can often not be freely exchanged across institutions  
87 due to the need for protection of the individual privacy, the utility of 'bringing the algorithm to the data'  
88 is becoming apparent. Technological solutions for this task have thus risen in popularity and exist in  
89 various forms. One of the most straightforward approaches is the so-called federated ML, where  
90 algorithms are simultaneously learned at different institutions and optimized through a privacy-  
91 preserving exchange of parameters. Other approaches for this task include the training of ML  
92 algorithms on temporarily combined data stored in working memory<sup>4</sup> or the more recently introduced  
93 'swarm-learning' approach<sup>5</sup>. One commonality of most ML algorithms, federated or not, is the  
94 assumption that all investigated observations (e.g. illness-affected individuals) represent the same  
95 underlying population. However, in biomedicine, this is rarely the case, as biological and technological  
96 factors frequently induce cohort-specific effects that limit the ability to identify reproducible biological  
97 findings. Multitask Learning (MTL) can address this issue through the simultaneous learning of  
98 outcome (e.g. diagnosis) associated patterns across datasets with dataset-specific, as well as shared,  
99 effects. Multi-task learning has numerous exciting application areas, such as comorbidity modeling,  
100 and has already been applied successfully for e.g. disease progression analysis<sup>6</sup>.

101 Here, we describe the development of dsMTL ('Federated Multi-Task Learning for DataSHIELD'), a  
102 package of the statistical software R, for **Federated Multi-Task Learning (FeMTL)** analysis (**Figure 1** ).  
103 dsMTL was developed for DataSHIELD<sup>7</sup>, a platform supporting the federated analysis of sensitive  
104 individual-level data that remains stored behind the data owner's firewall throughout analysis<sup>8</sup>. dsMTL  
105 includes three supervised and one unsupervised federated multi-task learning algorithms that extend

106 algorithms previously developed for non-federated analysis (for R implementations, see <sup>9,10</sup>).  
107 Specifically, the **dsMTL\_L21** approach allows for cross-task regularization, building on the popular  
108 LASSO method, in order to identify outcome-associated signatures with a reduced number of features  
109 shared across tasks. The non-federated version of this approach has previously been applied to  
110 simultaneously predict multiple oncological outcomes using gene expression data<sup>11</sup>. The **dsMTL\_trace**  
111 approach constrains the coefficient vectors in a low-dimensional space during the training procedure  
112 to penalize the complexity of task relationships, resulting in an improved generalizability of the models.  
113 In a non-federated implementation, this method has previously been used to predict the response to  
114 different drugs, and the identified models showed a high degree of interpretability in the context of  
115 the represented drug mechanism<sup>12</sup>. **dsMTL\_net** incorporates the task relationships that can be  
116 described as a graph, in order to improve biological interpretability. In a non-federated version, this  
117 technique has previously been used for the integrative analysis of heterogeneous cohorts<sup>13</sup> and for the  
118 prediction of disease progression<sup>14</sup>. The **dsMTL\_iNMF** approach is an unsupervised, integrative non-  
119 negative matrix factorization method that aims at factorizing the cohorts' data matrices into shared  
120 and dataset-specific components. Such modeling has been applied to explore dependencies in multi-  
121 omics data for biomarker identification<sup>10,15</sup>. In addition to the FeMTL methods, we also implemented  
122 a federated version of conventional Lasso (dsLasso)<sup>16</sup> in dsMTL package due to its wide usage in  
123 biomedicine and as a benchmark for testing the performance of the federated MTL algorithms.

124 To explore the utility of the dsMTL algorithms, we used a network comprising three servers. These  
125 servers hosted simulated data with variable degrees of cross-dataset heterogeneity, in order to test  
126 the ability of the MTL algorithms to suitably characterize shared and specific biological signatures. In  
127 addition, we analyzed actual RNA sequencing and microarray data across the three-server network, to  
128 show that the accurate analysis can be performed in acceptable runtime using dsMTL in real network  
129 latency.

130

131 **Results**

132 Here we show the results for two case studies. The first case study aims at demonstrating the utility of  
133 the supervised **dsMTL\_L21** algorithm to identify ‘heterogeneous’ target signatures across the data  
134 network. With ‘heterogeneous’ we describe signatures that involve the same features (e.g. genes) but  
135 with potentially differing signs (indicating differential directions of influences) across datasets. In  
136 contrast, ‘homogeneous’ signatures relate to the same features and signs across datasets. The second  
137 case study focuses on the unsupervised **dsMTL\_iNMF** method and explores the utility of the federated  
138 implementation, compared to the aggregation of local NMF models, to disentangle shared and cohort-  
139 specific components across datasets. For all case studies, we evaluated the signature identification  
140 accuracy as the major metric. For predictions of clinical outcomes, the prediction accuracy was also  
141 demonstrated.

142

143 *Case study 1 – distributed MTL for identification of heterogeneous target signatures*

144 With the aim to identify ‘heterogeneous’ signatures, we compared the performance of dsMTL\_L21,  
145 dsLasso and the bagging of glmnet models. As part of this, we explored the sensitivity of these methods  
146 to different sample sizes ( $n$ ) relative to the gene number ( $p$ ). **Figure 2** shows the resulting prediction  
147 performance and gene selection accuracy, each averaged over 100 repetitions. dsLasso showed the  
148 worst prediction performance in this heterogeneous setting, and dsMTL\_L21 slightly outperformed  
149 the aggregation of local models (glmnet). Similarly, the gene selection accuracy of dsLasso was inferior  
150 to that of dsMTL\_L21 and glmnet-bagging, which showed similar performance when the sample size is  
151 sufficiently large, e.g. the number of subjects approximately equal to the number of genes ( $n/p \sim 1$ ).  
152 However, with a decreasing  $n/p$  ratio, dsMTL\_L21 showed an increasing superiority over the other  
153 methods, especially for  $n/p=0.15$ , where the gene selection accuracy of dsMTL\_L21 was over 2.8 times  
154 higher than that of the bagging technique.

155

156 *Case study 2 – distributed iNMF for disentangling shared and cohort-specific signatures*

157 **Figure 3** shows the performance of distributed and aggregated local NMF methods for disentangling  
158 shared and cohort-specific signatures from multi-cohort data, given different ‘severities’ of the  
159 signature heterogeneity. For both types of signatures, dsMTL\_iNMF outperformed the ensemble of  
160 local NMF models for any heterogeneity severity setting. Notably, even with increasing heterogeneity,  
161 the accuracy of dsMTL\_iNMF to capture shared genes remained stable at approximately 100%,  
162 illustrating the robustness of dsMTL\_iNMF against the heterogeneity’s severity shown in **Figure 3c**. In  
163 contrast, for the ensemble of local NMF, the gene selection accuracy of the shared signature  
164 continuously decreased to approximately 50% (20% of outcome-associated genes were shared among  
165 cohorts), while the gene selection accuracy of cohort-specific signatures continuously increased to 75%  
166 (20% of outcome-associated genes were shared among cohorts ) as shown in **Figures 3a and 3b**.

167

168 *Efficiency of supervised dsMTL*

169 We aimed at determining the efficiency of supervised dsMTL using the real molecular data and the  
170 actual latency of a distributed network. Using a three-server scenario (see **Table 2 Supplementary**  
171 **Results**; two servers at the Central Institute of Mental Health, Mannheim; one server at BioQuant,  
172 Heidelberg University) we analyzed four case-control gene expression datasets of patients with  
173 schizophrenia and controls (median n=80; 8013 genes). **Supplementary Table 3** shows the comparison  
174 between dsLasso and mean-regularized dsMTL\_net, which were trained (cross-validation + training)  
175 and tested in approximately 8min and 10min, respectively, with the time-difference being due to the  
176 increased network access of dsMTL. The prediction accuracy of dsMTL was slightly higher than that of  
177 dsLasso, consistent with our previous study<sup>13</sup>. Regarding model interpretability, dsLasso captured a  
178 signature comprising 38 genes but could not distinguish shared and cohort-specific effects. Mean  
179 regularized dsMTL identified a signature with 10 genes shared among all cohorts, with 163 genes  
180 shared by two cohorts, as well as three cohort-specific signatures comprising 1532 genes.

181

182 *Efficiency of unsupervised dsMTL*

183 The cohorts and server information is shown in **Supplementary Table 4**. It took 34.9 minutes (1,003  
184 times network accesses) to train a dsMTL\_iNMF model with 5 random initializations (~7 min for each  
185 initialization). The factorization rank k=4 was selected as the optimal parameter. In **Supplementary**  
186 **Figure 1**, the objective curve illustrates that the training time was sufficient for model convergence. In  
187 this analysis, a shared signature comprising 473 genes between SCZ and BIP was identified, while two  
188 disease-specific signatures containing 37 genes for SCZ and 152 genes for BIP, respectively, were found.

189

190

191

192 **Discussion**

193 We here present dsMTL – a secure, federated multi-task learning package for the programming  
194 language R, building on DataSHIELD as an ecosystem for privacy-preserving and distributed analysis.  
195 Multi-task learning allows the investigation of research questions that are difficult to address using  
196 conventionalML, such as the identification of heterogeneous, albeit related, signatures across datasets.  
197 The implementation of a privacy-preserving framework for the distributed application of MTL is an  
198 essential requirement for the large-scale adoption of MTL. Using such a distributed server setup, we  
199 demonstrate the applicability and utility of dsMTL to identify biomarker signatures in different settings.  
200 For applications where the target biomarker signatures are different, but relate to an overlapping set  
201 of features (explored here as the ‘heterogeneous’ case), conventional machine learning would not be  
202 a meaningful algorithm choice. We show that MTL is able to identify the target signatures with high  
203 confidence and may thus be a reasonable choice for a diverse set of interesting analyses. As mentioned  
204 above, a particularly noteworthy application is comorbidity modeling, where the target signatures

205 index the shared (although potentially heterogeneously manifested) biology of multiple, clinically  
206 comorbid conditions. Such analyses could potentially be a powerful, machine learning-based extension  
207 of comorbidity modeling approaches based on univariate statistics that have already been very useful  
208 for characterizing the shared biology of comorbid illness<sup>17</sup>. We show that unsupervised MTL can  
209 disentangle the shared from cohort-specific effects, demonstrating its potential utility for comorbidity  
210 analysis. Other applications for this method include the analysis of biological patterns shared across  
211 clinical symptom domains, between clinical and demographic characteristics, or with digital measures,  
212 such as ecological momentary assessments.

213 The use of dsMTL follows the concept of the so-called “freely composing script” in the DataSHIELD  
214 ecosystem. It organizes a given dsMTL workflow as a free composition of dsMTL, DataSHIELD, and local  
215 R commands (e.g. R base functions, customer-defined functions and CRAN packages) into a script, such  
216 that the geo-distribution of datasets and the federated computation are transparent to users. This  
217 concept is similar to that of the “freely composing apps” used in a recently presented federated ML  
218 application<sup>18</sup>, which allows flexible scheduling of functions in the form of apps and improves the  
219 federated data analysis flexibility for users. In addition to dsMTL, other packages in the DataSHIELD  
220 ecosystem exist for e.g. “big data” storage and management<sup>19</sup>, various statistical tests<sup>7,19</sup> and deep  
221 learning<sup>19,20</sup>.

222 Interesting future developments of the dsMTL approach could include the implementation of  
223 asynchronous communication, which provides a probabilistically approximate solution but faster  
224 convergence<sup>21,22</sup>. Furthermore, integration of other popular systems for ML, such as tensorflow<sup>23</sup>, for  
225 which interfaces with the R language already exist, would provide valuable additions to the DataSHIELD  
226 system. Finally, a noteworthy consideration is an architecture underlying the distributed data  
227 infrastructure. DataSHIELD builds on a centralized (“client-server”) architecture and each data provider  
228 needs to install a well-configured data warehouse. Such infrastructure is suitable for long-term  
229 collaboration scenarios and large consortia projects that conduct a broad spectrum of complex  
230 analyses requiring high flexibility. However, in other scenarios that require more temporary and easy-

231 compute collaboration setups, a server-free or decentralized architecture<sup>24</sup> might be more suitable,  
232 because the cost of data provider for participating is low.

233 In conclusion, the dsMTL library for the programming language R provides an easy-to-use framework  
234 for privacy-preserving, federated analysis of geographically distributed datasets. Due to its ability to  
235 disentangle shared and cohort-specific effects across these datasets, dsMTL has numerous interesting  
236 application areas, including comorbidity modeling and translational research focused on the  
237 simultaneous prediction of different outcomes across datasets.

238

239

240 **Methods**

241 Modeling

242 All methods part of dsMTL share the identical form,

$$\min_{\theta} \mathcal{L}(\theta) + \lambda S(\theta) + C \aleph(\theta)$$

243 where  $\mathcal{L}(\theta)$  is the data fitting term (or loss function), the major determinant of the solutions obtained  
244 from model training.  $\aleph(\theta)$  and  $S(\theta)$  are the penalties of  $\theta$  with the aim to incorporate the prior  
245 information.  $\aleph(\theta)$  is a non-smooth function and able to create sparsity, while  $S(\theta)$  is smooth.  $\lambda$  and  $C$   
246 are the hyper-parameters to control the strength of the penalties. More technical details can be found  
247 in the supplementary methods.

248 In dsMTL, two approaches for sharing information across cohorts are included, 1) shared parameters  
249 and 2) cross-task regularization, leading to a slightly different distributed computation. The shared  
250 parameters are estimated using all cohorts. For cross-task regularization, the cohort-specific  
251 parameters are estimated using only the local data, and then tuned by considering parameters from  
252 other cohorts.

254 Efficiency

255 Most dsMTL methods aim at training an entire regularization tree. The determination of the  $\lambda$   
256 sequence controls the tree's growth and is essential for computational speed. The  $\lambda$  sequence should  
257 be accurately scaled to both capture the highest posterior and avoid overwhelming computations.  
258 Inspired by a previous study<sup>25</sup>, we estimate the largest and smallest  $\lambda$  from the data by characterizing  
259 the optima of the objective using the first-order optimal condition and then interpolate the entire  $\lambda$   
260 sequence on a log scale (see supplementary methods for more details). In addition, several options are  
261 provided to improve the speed of the algorithms by decreasing the precision of the results, i.e., 1) the  
262 number of digits of parameters for transformation can be specified to reduce the network latency; 2)  
263 several termination rules are provided, some of which are relaxed; 3) the depth of the regularization  
264 tree can be shortened. More details can be found in supplementary methods.

265 Besides the efficiency of the federated ML/MTL methodology, the import/export of “big data” cohorts  
266 is also crucial for computational efficiency, where e.g. uncompressed GWAS data requires tens of  
267 gigabytes, leading to time-consuming data import. dsMTL was designed to support a wide variety of  
268 data types. For this, an architecture package resourcer<sup>19</sup> developed by the DataSHIELD community was  
269 incorporated to facilitate the efficient import and export of large-scale datasets in compressed formats.  
270 For example, in DataSHIELD, GWAS data of the PLINK file formats can be read and processed using the  
271 software PLINK<sup>26</sup> as the backend<sup>19</sup>.

272 Security

273 dsMTL was developed based on DataSHIELD<sup>8</sup>, which provides comprehensive security mechanisms not  
274 specific to machine learning applications. For example, 1) DataSHIELD requires the data analysis to  
275 only occur behind the firewall; 2) each server is only allowed to communicate with a set of clients with  
276 fixed IP addresses; 3) the network communication is protected by an SSL protocol; 4) an R parser<sup>8</sup>  
277 implemented on the server rejects the calling of unwanted functions; and 5) the so-called ‘disclosure  
278 control’<sup>8</sup> on the server ensures that the returned response does not contain any disclosive information.

279 In addition, several permissions can be set by the data providers to fully control the usage of their data.

280 These permissions describe the degree of accessibility of data and functions on the server i.e. “*which*

281 *users can perform what actions on what data*”. In an extremely secure example, a user could be

282 granted to check the summary of a given dataset but cannot perform any actions because no functions

283 were granted. With these settings, DataSHIELD allows customizing the security protection strategies

284 according to the specific requirements of the applications. For statistical and machine learning analyses,

285 DataSHIELD assumes that summary statistics are safe to share.

286 dsMTL inherits all these security mechanisms. In addition, we considered potential ML-specific privacy

287 leaks, such as membership inference attacks<sup>27</sup> and model inverse attacks<sup>28</sup>. Inverse attacks aim at

288 extracting the individual observation-level information from the models. Membership inference

289 attempts to decide if an individual was included in a given training set using the model. All these

290 techniques require a complete model for inference. Since multi-task learning returns multiple matrices,

291 returning an incomplete model could be one strategy against these attacks. For example, dsMTL\_iNMF

292 in dsMTL only returns the homogenous matrix (H), whereas the cohort-specific components ( $V_k, W_k$ )

293 never leave the server. For example, in a two-server scenario, one (H) out of five output matrices is

294 transmitted between the client and the servers. With such an incomplete model, inverse construction

295 of the raw data matrix becomes difficult, and the risk of an inverse attack and membership inference

296 is reduced. For most biomedical analyses, the H matrix is sufficient for subsequent studies. In addition,

297 if the analyst was authorized to access the raw data of the server, the so-called “data key mechanism”

298 (see supplement) would allow the analyst to retrieve all component matrices. For supervised multi-

299 task learning methods in dsMTL, all models have to be aggregated within the clients, and thus we

300 suggest the data providers enable the option on the server that rejects a returned coefficient vector

301 containing parameter numbers exceeding the number of subjects. In this way, the model is not

302 saturated and more robust to an inverse attack.

303 Proof of concept with simulation and actual data

304 Two case studies and speed-tests were conducted to demonstrate the suitability of dsMTL methods to  
305 analyze heterogeneous cohorts, compared to federated ML methods and ensemble of local models  
306 regarding the prediction performance, interpretability and computational speed. An overview of  
307 methodological aspects related to the case studies is detailed below. For an extensive methodological  
308 description, please see the supplementary Methods.

309 **Case study 1.** In this case study, the heterogeneous cohorts were generated with the same set of  
310 outcome-associated genes. These however showed different directionality of their respective  
311 associations with the outcome. A three-server scenario was simulated. 150 out of 500 features with  
312 random signs across cohorts were simulated. Seven tests were created for simulating different n/p  
313 ( $\frac{\text{sample size}}{\text{gene number}}$ ) ratios. The n/p ratio was  $\{1.2, 1, 0.9, 0.6, 0.5, 0.3, 0.15\}$  with the number of subjects  
314  $\{600, 500, 450, 300, 250, 150, 75\}$  for each test. 500 genes were created for each server. The test  
315 sample consisted of 200 subjects for each server. Data were generated as follows:

316 Given gene number  $p = 500$ , the models of three cohorts were  $\{w^{(1)}, w^{(3)}, w^{(3)}\}$  where  $w^{(\cdot)} = p \times 1$ .  
317 A shared signature comprising 150 genes was generated for each  $w^{(\cdot)}$  but with random signs,  $w^{(\cdot)}_i =$   
318  $\begin{cases} 2 \times (\rho - 0.5) \times N(1, 0.1) & 1 < i < 150 \\ 0 & \text{others} \end{cases}, \rho \sim \text{Bernoulli}(\frac{1}{2})$ . The expression values of each subject  
319 across cohorts were generated as  $x = 1 \times p$  where  $x_j \sim N(0, 1)$ . The numeric outcome (e.g. symptom  
320 severity)  $y = xw^{(i)}$  in cohort  $i$  was standardized in a normal distribution  $N(0, 1)$ , then model-  
321 irrelevant noise with 50% of the variance of the true signal was added  $y = y + N(0, 0.5)$ .

322 dsMTL\_L21 and dsLasso were trained as the federated learning system, and the hyper-parameter was  
323 selected using 10 fold in-cohort cross-validation. For glmnet, the ensemble technique was only applied  
324 on the gene selection due to the consistent gene set of their signatures. The mean squared error (mse)  
325 was used as the measure of prediction performance. To account for the sampling variance, we  
326 repeated each analysis 100 times.

327 **Case study 2.** In this case study, two heterogeneous RNA-seq cohorts were created to simulate a  
328 comorbidity analysis, where the genes were separated to be part of either a shared signature among  
329 cohorts, cohort-specific signatures or diagnosis-unassociated genes. The dsMTL\_iNMF was compared  
330 to the ensemble of local NMF regarding the selection accuracy of shared/cohorts-specific genes, in  
331 particular impacted by the severity of heterogeneity. Here the severity of heterogeneity refers to the  
332 proportion of the genes harbored by the shared signature over all diagnosis-associated genes. The data  
333 simulation protocol for RNA-seq data can be found in the **Supplementary Methods**.

334 A two-server scenario was simulated. As shown in **Supplementary Table 1**, for the data of each server,  
335 1000 genes and 200 subjects were simulated, 50% of the genes were diagnosis-unassociated and the  
336 remaining genes were part of the disease signature. The genes comprised by shared signatures were  
337 identical for data of two servers, and the genes comprised by cohort-specific signatures did not overlap.  
338 The case-control ratio was balanced for each server. Four tests were performed by varying the  
339 proportion of genes in the shared signature over all diagnosis-associated genes from 20% to 80%.

340 The training of dsMTL\_iNMF results in three outputs related to the original input data: the shared gene  
341 'exposure' (H), cohort-specific gene 'exposure' (V) and sample 'exposure' (W). We measured the  
342 association between the sample exposure and the diagnosis as the weight of each latent factor. The  
343 shared( or specific) gene signature was identified as the weighted summation of the shared (or specific)  
344 gene exposures over latent factors. To quantify the important genes related to a given signature, we  
345 binarized the gene signature according to the mean (0-1 vector, values larger than the mean were  
346 assigned). To assess the performance of the gene identification, we associated the selected genes set  
347 with the ground truth (0-1 vector, signature genes were 1). The assessment was applied to shared and  
348 cohort-specific genes in parallel. Based on this metric, three gene sets were derived as output from  
349 dsMTL\_iNMF, called dsMTL\_iNMF-H, dsMTL\_iNMF-V1 and dsMTL\_iNMF-V2, and these related to the  
350 shared, cohort 1 specific and cohort 2 specific gene signature, respectively. The same strategy was  
351 applied to analyze the ensemble of local NMF models. For each cohort, the specific gene signature was  
352 the weighted summation of gene exposure over latent factors, and then binarized as the specific gene

353 set (called local-NMF1 and local-NMF2). The shared gene signature was identified as the sum of the  
354 specific gene signature over cohorts, and then binarized as the shared gene set(NMF-bagging). We  
355 then compared 1) NMF-bagging and dsMTL\_iNMF-H for the accuracy related to the isolation of shared  
356 genes; 2) dsMTL\_iNMF-V1 and local-NMF1 as well as dsMTL\_iNMF-V2 and local-NMF2 for the accuracy  
357 of isolating cohort-specific genes.

358 **Computational speed of supervised dsMTL.** We aimed at identifying the efficiency of supervised  
359 dsMTL using real molecular data and given the real network latency. Four independent schizophrenia  
360 case-control cohorts were used for this analysis. The training cohorts consisted of three datasets  
361 comprising prefrontal cortex gene expression data (available from the GEO repository under accession  
362 numbers GSE53987, GSE21138 and GSE35977). A detailed description of these datasets can be found  
363 in their respective original publications<sup>29-31</sup>. The dataset used for algorithm testing was from the HBCC  
364 (n=422) cohort comprising genome-wide gene expression data quantified by microarray (dbGAP ID:  
365 phs000979.v3.p2). A detailed description of this dataset can be found in the original publication<sup>32</sup>. As  
366 shown in **Supplementary Table 2**, three servers were used for training algorithms. Two servers were  
367 held at the Central Institute of Mental Health, Mannheim while the third was positioned at the  
368 BioQuant institute, Heidelberg.

369 Using this data, we repeated a previously described analysis<sup>13</sup>, in order to evaluate computational  
370 speed in a federated analysis setting. Here we show the formulation of the mean regularized MTL using  
371 dsMTL\_net:

372 The cohort-level batch effect was assumed to be Gaussian noise affecting the true coefficient of gene  
373 i and cohort j  $w_{ij} = w_i + \epsilon_j$ ,  $\epsilon_j \in N(\mu, \sigma)$ . Hence, the average model  $\bar{w}_i$  across cohorts was an  
374 unbiased estimator for the true coefficient, and therefore the squared penalty  $|w_{ij} - \bar{w}_i|^2$  was  
375 incorporated to penalize the departure of each model j to the mean. The complete formulation was

$$376 \min_W \sum_{k=1}^3 \sum_{i=1}^{n_k} \frac{1}{n_k} \log(1 + e^{-Y_i^{(k)}(X_i^{(k)}W_{:,k})}) + \lambda ||W||_1 + C ||WG||_2^2,$$

377

$$\text{where } G = \begin{bmatrix} \frac{2}{3} & 0 & \frac{-1}{3} & \frac{2}{3} & \frac{-1}{3} & 0 \\ \frac{-1}{3} & \frac{2}{3} & 0 & 0 & \frac{2}{3} & \frac{-1}{3} \\ \frac{1}{3} & \frac{1}{3} & 0 & 0 & \frac{2}{3} & \frac{-1}{3} \\ 0 & \frac{-1}{3} & \frac{2}{3} & \frac{-1}{3} & 0 & \frac{2}{3} \end{bmatrix}$$

378

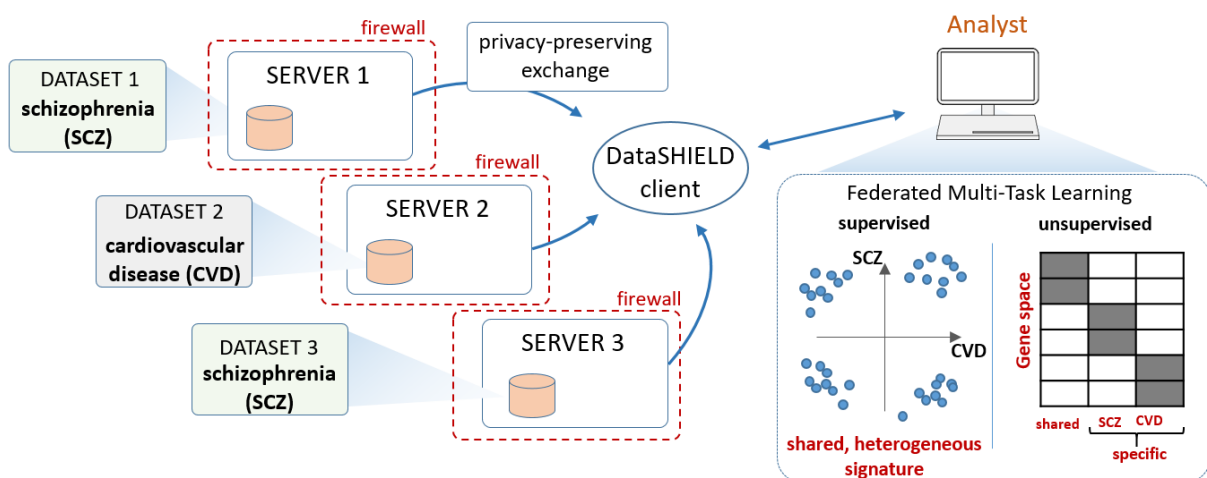
379 **Computational speed of unsupervised dsMTL.** Here, we analyzed the time efficiency in applying  
380 dsMTL\_iNMF on two real datasets based on the real network latency. Two processed RNA-seq case-  
381 control cohorts comprising patients with schizophrenia (GSE164376<sup>33</sup> ) and bipolar disorder  
382 (GSE134497<sup>34</sup>) were retrieved from the GEO database and converted into a matrix format for the  
383 analysis. As shown in **Supplementary Table 4**, the data were stored on servers in Mannheim and  
384 Heidelberg.

385

386

387

388 **Figures**

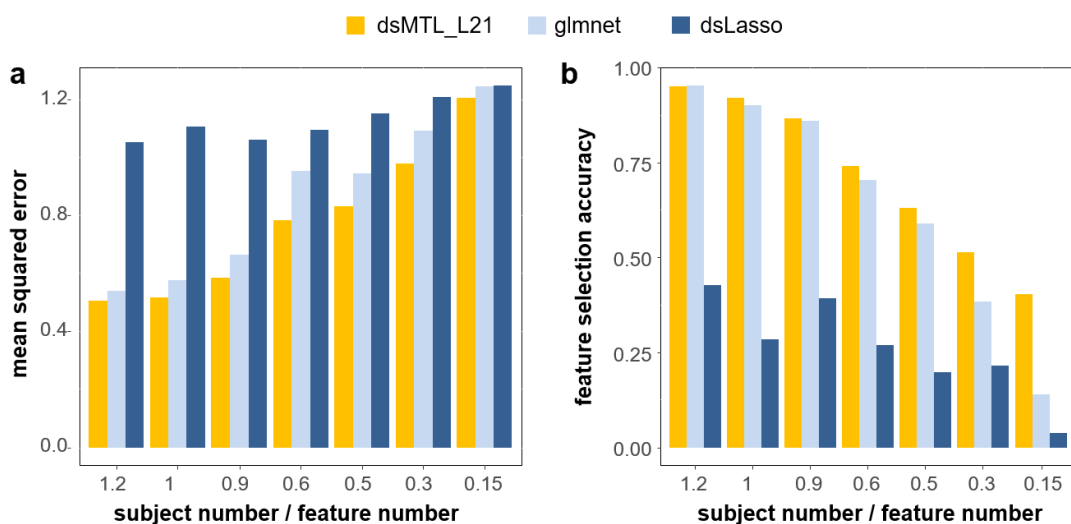


389

390 **Figure 1. Schematic illustration of dsMTL using comorbidity modeling of schizophrenia and**  
391 **cardiovascular disease as an example.** Multiple datasets stored at different institutions are used as a  
392 basis for federated MTL. dsMTL was developed in the DataSHIELD ecosystem, which provides

393 functionality regarding data management, transmission and security. Data are analyzed behind a given  
394 institution's firewall and only algorithm parameters that do not disclose personally identifiable  
395 information are exchanged across the network. dsMTL contains algorithms for supervised and  
396 unsupervised multi-task machine learning. The former aims at identifying shared, but potentially  
397 heterogeneous signatures across tasks (here, diagnostic classification for schizophrenia and  
398 cardiovascular disease). Unsupervised learning separates the original data into shared and cohort-  
399 specific components, and aims at revealing the corresponding outcome-associated biological profiles.

400



401

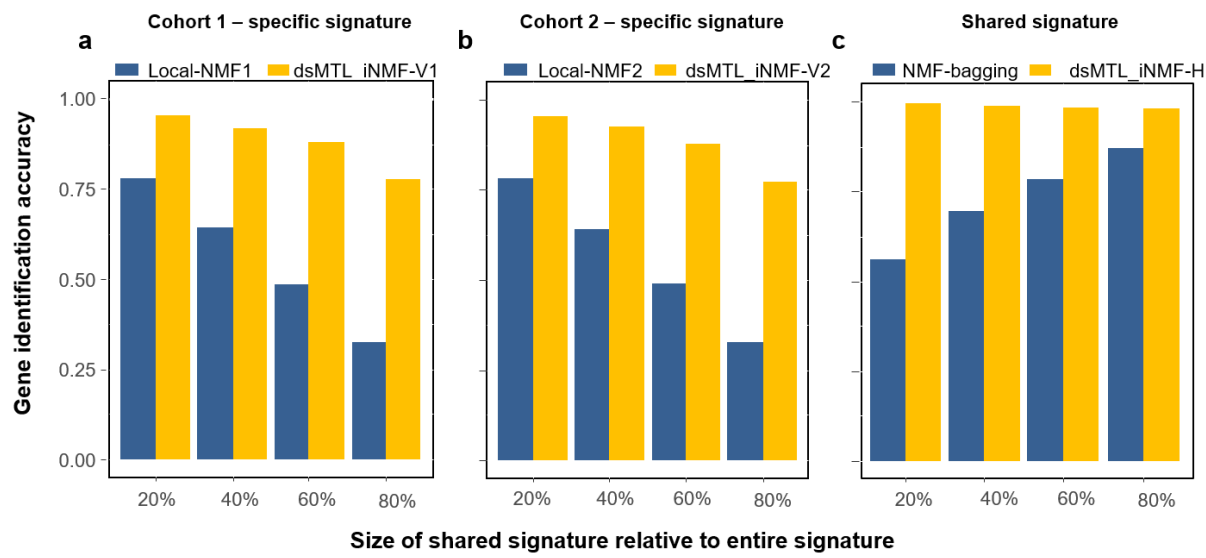
402 **Figure 2. Analysis of 'heterogeneous' signatures of continuous outcomes in simulated data stored**  
403 **on three servers.** The figure shows the **a)** prediction accuracy expressed as the mean squared error  
404 and **b)** the feature selection accuracy for different subject/feature number ratios. The respective  
405 values were averaged across the three servers, and across 100 repetitions, in order to account for the  
406 effect of sampling variability.

407

408

409

410



411

412 **Figure 3. The gene identification accuracy for shared and specific signatures using simulated data. a)**  
413 the identification accuracy of important genes for cohort 1. **b)** the identification accuracy of important  
414 genes for cohort 2. **c)** the identification accuracy of genes comprised in the shared signature. Local-  
415 NMF1 and Local-NMF2 were the cohort-specific gene sets identified by local NMF, which were  
416 combined into “NMF-bagging” for the shared gene set. dsMTL\_iNMF-H was the predicted shared gene  
417 set using dsMTL\_iNMF. dsMTL\_iNMF-V1 and dsMTL\_iNMF-V2 were the predicted cohort-specific gene  
418 sets identified using dsMTL\_iNMF (see Supplementary Figure 1). The proportion of genes harbored by  
419 the shared signature was varied from 20% to 80% illustrating the impact of the heterogeneity severity.  
420 The model was trained using rank=4 as model parameter. The results for a broader spectrum of rank  
421 choices can be found in **Supplementary Figure 2** illustrating that the superior performance of  
422 dsMTL\_iNMF was not due to the choice of ranks.

423

424

425 **Acknowledgements**

426 This study was supported by the Deutsche Forschungsgemeinschaft (DFG), SCHW 1768/1-1 and the  
427 German Federal Ministry of Education and Research (BMBF, grants 01KU1905A and 01ZX1904A).

428

429 **Competing interests**

430 AML has received consultant fees from: Boehringer Ingelheim, Elsevier, Brainsway, Lundbeck Int.  
431 Neuroscience Foundation, Lundbeck A/S, The Wolfson Foundation, Bloomfield Holding Ltd, Shanghai  
432 Research Center for Brain Science, Thieme Verlag, Sage Therapeutics, v Behring Röntgen Stiftung,  
433 Fondation FondaMental, Janssen-Cilag GmbH, MedinCell, Brain Mind Institute, Agence Nationale de la  
434 Recherche, CISSN (Catania Internat. Summer School of Neuroscience), Daimler und Benz Stiftung,  
435 American Association for the Advancement of Science, Servier International. Additionally he has  
436 received speaker fees from: Italian Society of Biological Psychiatry, Merz-Stiftung, Forum Werkstatt  
437 Karlsruhe, Lundbeck SAS France, BAG Psychiatrie Oberbayern, Klinik für Psychiatrie und  
438 Psychotherapie Ingolstadt, med Update GmbH, Society of Biological Psychiatry, Siemens Healthineers,  
439 Biotest AG. All other authors have no potential conflicts of interest.

440

441 **References**

- 442 1. Jahanshad N, Kochunov PV, Sprooten E, et al. Multi-site genetic analysis of diffusion images  
443 and voxelwise heritability analysis: A pilot project of the ENIGMA–DTI working group.  
444 *NeuroImage*. 2013;81:455-469.
- 445 2. Schizophrenia Working Group of the Psychiatric Genomics C. Biological insights from 108  
446 schizophrenia-associated genetic loci. *Nature*. 2014;511(7510):421-427.
- 447 3. Kochunov P, Jahanshad N, Sprooten E, et al. Multi-site study of additive genetic effects on  
448 fractional anisotropy of cerebral white matter: comparing meta and megaanalytical  
449 approaches for data pooling. *NeuroImage*. 2014;95:136-150.
- 450 4. Carter KW, Francis RW, Carter K, et al. ViPAR: a software platform for the Virtual Pooling and  
451 Analysis of Research Data. *International journal of epidemiology*. 2016;45(2):408-416.
- 452 5. Warnat-Herresthal S, Schultze H, Shastry KL, et al. Swarm Learning for decentralized and  
453 confidential clinical machine learning. *Nature*. 2021;594(7862):265-270.
- 454 6. Zhou J, Liu J, Narayan VA, Ye J, Alzheimer's Disease Neuroimaging I. Modeling disease  
455 progression via multi-task learning. *NeuroImage*. 2013;78:233-248.
- 456 7. Gaye A, Marcon Y, Isaeva J, et al. DataSHIELD: taking the analysis to the data, not the data to  
457 the analysis. *International journal of epidemiology*. 2014;43(6):1929-1944.

458 8. Wilson RC, Butters OW, Avraam D, et al. DataSHIELD – New Directions and Dimensions. *Data  
459 Science Journal*. 2017;16.

460 9. Cao H, Zhou J, Schwarz E. RMTL: An R Library for Multi-Task Learning. *Bioinformatics*. 2018.

461 10. Yang Z, Michailidis G. A non-negative matrix factorization method for detecting modules in  
462 heterogeneous omics multi-modal data. *Bioinformatics*. 2016;32(1):1-8.

463 11. Xu Q, Xue H, Yang Q. Multi-platform gene-expression mining and marker gene analysis.  
464 *International journal of data mining and bioinformatics*. 2011;5(5):485-503.

465 12. Yuan H, Paskov I, Paskov H, Gonzalez AJ, Leslie CS. Multitask learning improves prediction of  
466 cancer drug sensitivity. *Scientific reports*. 2016;6:31619.

467 13. Cao H, Meyer-Lindenberg A, Schwarz E. Comparative Evaluation of Machine Learning  
468 Strategies for Analyzing Big Data in Psychiatry. *International journal of molecular sciences*.  
469 2018;19(11).

470 14. Zhou J, Yuan L, Liu J, Ye J. A multi-task learning formulation for predicting disease  
471 progression. 2011:814.

472 15. Fujita N, Mizuarai S, Murakami K, Nakai K. Biomarker discovery by integrated joint non-  
473 negative matrix factorization and pathway signature analyses. *Scientific reports*.  
474 2018;8(1):9743.

475 16. Tibshirani R. Regression shrinkage and selection via the lasso. *Journal of the Royal Statistical  
476 Society Series B (Methodological)*. 1996:267-288.

477 17. Lichtenstein P, Yip BH, Björk C, et al. Common genetic determinants of schizophrenia and  
478 bipolar disorder in Swedish families: a population-based study. *The Lancet*.  
479 2009;373(9659):234-239.

480 18. Matschinske J, Späth J, Nasirigerdeh R, et al. The FeatureCloud AI Store for Federated  
481 Learning in Biomedicine and Beyond. *arXiv preprint arXiv:210505734*. 2021.

482 19. Marcon Y, Bishop T, Avraam D, et al. Orchestrating privacy-protected big data analyses of  
483 data from different resources with R and DataSHIELD. *PLoS computational biology*.  
484 2021;17(3):e1008880.

485 20. Lenz S, Hess M, Binder H. Deep generative models in DataSHIELD. *BMC Med Res Methodol*.  
486 2021;21(1):64.

487 21. Zhang C, Liu J. Distributed Learning Systems with First-Order Methods. *Foundations and  
488 Trends® in Databases*. 2020;9(1):1-100.

489 22. Xie L, Baytas IM, Lin K, Zhou J. Privacy-Preserving Distributed Multi-Task Learning with  
490 Asynchronous Updates. 2017:1195-1204.

491 23. Dahl M, Mancuso J, Dupis Y, et al. Private machine learning in tensorflow using secure  
492 computation. *arXiv preprint arXiv:181008130*. 2018.

493 24. Warnat-Herresthal S, Schultze H, Shastry KL, et al. Swarm Learning as a privacy-preserving  
494 machine learning approach for disease classification. 2020.

495 25. Friedman J, Hastie T, Tibshirani R. Regularization Paths for Generalized Linear Models via  
496 Coordinate Descent. *Journal of Statistical Software*. 2010;33(1).

497 26. Purcell S, Neale B, Todd-Brown K, et al. PLINK: a tool set for whole-genome association and  
498 population-based linkage analyses. *American journal of human genetics*. 2007;81(3):559-575.

499 27. Hu H, Salcic Z, Dobbie G, Zhang X. Membership Inference Attacks on Machine Learning: A  
500 Survey. *arXiv preprint arXiv:210307853*. 2021.

501 28. Fredrikson M, Lantz E, Jha S, Lin S, Page D, Ristenpart T. Privacy in pharmacogenetics: An  
502 end-to-end case study of personalized warfarin dosing. Paper presented at: 23rd {USENIX}  
503 Security Symposium ({USENIX} Security 14)2014.

504 29. Lanz TA, Reinhart V, Sheehan MJ, et al. Postmortem transcriptional profiling reveals  
505 widespread increase in inflammation in schizophrenia: a comparison of prefrontal cortex,  
506 striatum, and hippocampus among matched tetrads of controls with subjects diagnosed with  
507 schizophrenia, bipolar or major depressive disorder. *Translational psychiatry*. 2019;9(1):151.

508 30. Tang B, Capitao C, Dean B, Thomas EA. Differential age- and disease-related effects on the  
509 expression of genes related to the arachidonic acid signaling pathway in schizophrenia.  
510 *Psychiatry research*. 2012;196(2-3):201-206.

511 31. Chen C, Cheng L, Grennan K, et al. Two gene co-expression modules differentiate psychotics  
512 and controls. *Mol Psychiatry*. 2013;18(12):1308-1314.

513 32. Fromer M, Roussos P, Sieberts SK, et al. Gene expression elucidates functional impact of  
514 polygenic risk for schizophrenia. *Nature neuroscience*. 2016;19(11):1442-1453.

515 33. A; K, R; K. GSE164376 dataset.  
516 <https://www.ncbi.nlm.nih.gov/geo/query/acc.cgi?acc=GSE164376>. Published 2021.  
517 Accessed.

518 34. Kathuria A, Lopez-Lengowski K, Vater M, McPhie D, Cohen BM, Karmacharya R.  
519 Transcriptome analysis and functional characterization of cerebral organoids in bipolar  
520 disorder. *Genome medicine*. 2020;12(1):34.

521